Experimental Studies in Helicopter Vertical Climb Performance

Final Report for NASA Grant NAG 2-783

Robert M. McKillip, Jr.

February 1996

Abstract

Data and analysis from an experimental program to measure vertical climb performance on an eight-foot model rotor are presented. The rotor testing was performed using a unique moving-model facility capable of accurately simulating the flow conditions during axial flight, and was conducted from July 9, 1992 to July 16, 1992 at the Dynamic Model Track, or "Long Track", just prior to its demolition in August of 1992. Data collected during this brief test program included force and moment time histories from a sting-mounted strain gauge balance, support carriage velocity, and rotor rpm pulses. In addition, limited video footage (of marginal use) was recorded from smoke flow studies for both simulated vertical climb and descent trajectories. Analytical comparisons with these data include a series of progressively more detailed calculations ranging from simple momentum theory, a prescribed wake method, and a free-wake prediction.

Introduction

U.S. Army requirements for vertical rate of climb performance were emphasized in the Utility Tactical Transport Aircraft System (UTTAS) and Advanced Attack Helicopter (AAH) program specifications, due to a recognized importance that this metric plays in survivability of both aircraft in military operations [1]. Certain flight test measurements, though rather inaccurate at low climb rates, have indicated that simple momentum theory over-predicts the power required to attain specified levels of climb rate (e.g., Reference 2). Such over-predictions can in turn place increased requirements on installed power for a given aircraft, which translate into higher fly-away costs for a new design. While some techniques attempt to account for this error through semi-empirical methods [3], they are hampered by a fundamental scatter in data from flight test. These data are subject to variable winds, pilot skill in sustaining a vertical climb path, and ability to maintain a steady climb rate. In addition, the power increments at low climb rates are often buried in the noise present in the instrumentation available.

The goal of the test program described here was to conduct a series of controlled tests using a moving model rotor in axial flight. Use of the Dynamic Model Track (or, Long Track) at Princeton University was central to the accurate collection of power and thrust data in a turbulence-free test environment. These test data also included some limited flow visualization studies to provide increased understanding of the wake structure in this important flight regime. These flow visualization studies, however, proved to be of limited value, and were unable to be improved upon due to the imminent destruction of the test facility.

Facility Description

The Dynamic Model Track, or "Long Track", was a unique facility located on the Forrestal Campus at Princeton University. Originally designed for studying flight dynamics of helicopter and V/STOL systems, it was extended to 750 feet in length to provide adequate data records for force and moment measurement on powered models at a variety of simulated flight speeds. The Long Track had been recently upgraded in instrumentation capability, with a six-component sting balance coupled to a high-bandwidth digital data acquisition system [4]. Precise control of forward

speed was maintained through electronic control of a hydraulically driven carriage support system on a monorail track. Use of moving helicopter models at low speeds could provide accurate simulation of boundary conditions in ground effect, operation in zero turbulence, reduced power requirements, and precise velocity control. In addition, the large track cross-section size of 30' x 30' eliminated the requirements for wall corrections to the test data. The vertical climb performance experiments that were conducted under this test program were designed to directly address a deficiency in accurate rotor data in this flight regime. Extraction of reliable information from flight test data in these conditions is extremely difficult, due to the lack of experimental control often possible in such testing. These data resulting from such a fundamental study, conducted in a turbulence-free facility on an isolated rotor, should provide a valuable reference source for correlation with design and analysis codes in industry and government.

Rotor Model

The experimental program made use of an existing 8-foot diameter hingeless rotor model, used in previous studies on ground effect aerodynamics [5] and compound helicopter configurations [6]. Since this model rotor was originally designed for Froude-scale testing, the experiment described here was at a reduced tip speed. Collective pitch was mechanically adjusted and locked in place between runs, as necessary, with cyclic inputs set to zero throughout. This model was mounted at 90 degrees from its conventional orientation in order to use the longitudinal carriage motion to simulate vertical climb over a range of climb velocities. This reorientation of the model also allowed the use of the "roll" moment measurement of the 6-component strain gauge sting balance to be oriented parallel to the model rotor shaft, providing increased sensitivity for measurement of rotor torque. Unfortunately for the latter third of the test data, this balance channel saturated the capability of the digital data acquisition system (a fact discovered at the conclusion of the test program), and hence rotor power data presented here is only accurate for the lower two rotor blade collective pitch settings. Flow visualization studies using a carriage-mounted smoke system were also used to complement the sting balance data, and were to provide additional details of the structure of the rotor wake vortex in the climb state. This system used a two component mixture of sulfur dioxide and anhydrous ammonia, mixed together at the smoke probe tip, to provide high density smoke filaments to aid in tracking the rotor wake in axial flight. A carriage-mounted 8mm video camera was used to record these smoke flow images as part of the data collected for this experiment. A schematic of the model orientation on the carriage and the smoke probe placement is given in Figure 1. Parameters of the model rotor geometry and blade properties are given in Table 1, taken from Ref. 6.

Data Acquisition and Processing

Data for the tests described here came from five sources: a 1/rev optical pickup on the rotor shaft for recording rotor shaft speed; a carriage-mounted tachometer/generator for measuring carriage velocity (and hence vertical climb and descent velocity); an optical pickup on the hydraulic carriage for recording when the carriage passed in from of a steel I-beam support post, the latter spaced exactly 10 feet apart along the length of the building; a six-component strain gauge balance system, for recording rotor loads in hover and axial translation; and an 8mm video camera for recording images of the rotor operation, with and without smoke introduced via probes above the rotor disk. These data were recorded in two different formats: as digitized time histories transmitted from a serial digital data acquisition unit, and as a Pulse-Width-Modulated (PWM) serial data stream on the audio track of the 8mm video recorder unit. All of the data described in this report's Appendix were from the digital data unit.

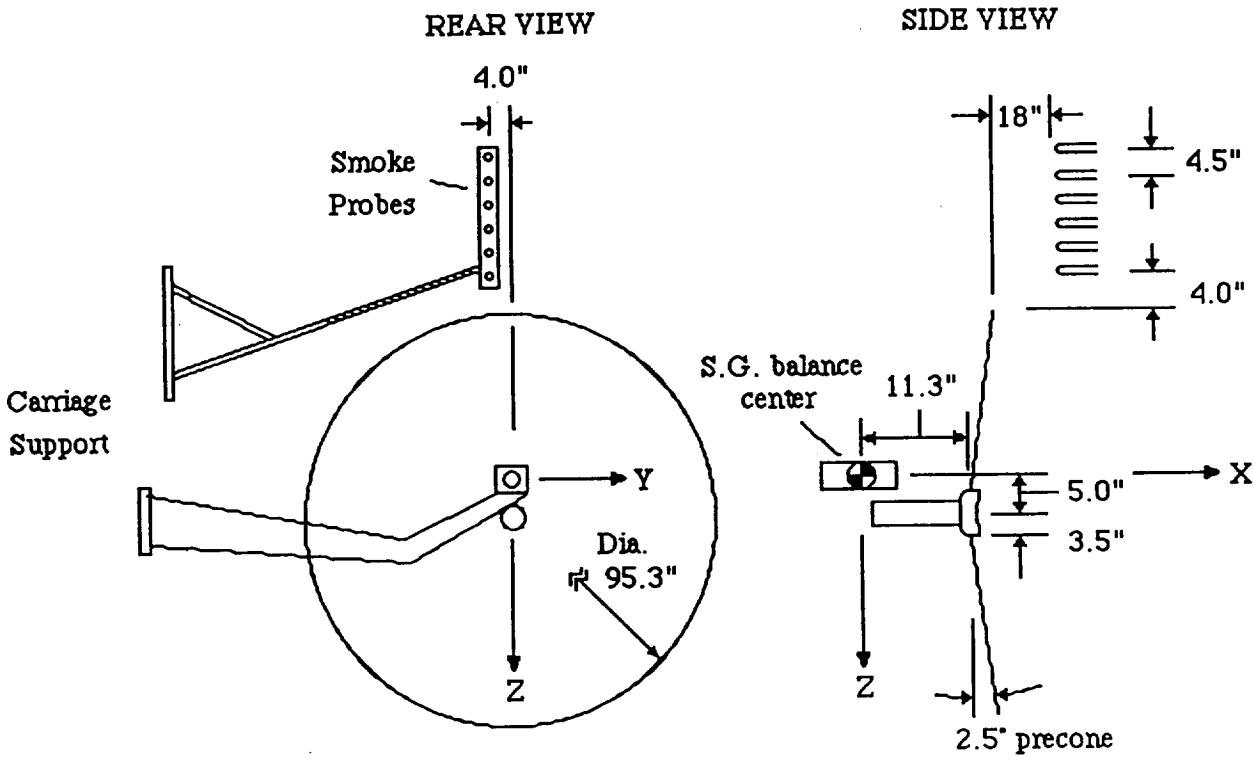

Figure 1: Model Rotor Orientation for Vertical Climb Tests

Table 1: Model Rotor Parameters

Number of blades	4
Radius	2.44m (4 ft)
Root Cutout	10% radius
Blade Chord	0.0635m (2.5 in)
Solidity	0.0663
Airfoil	NACA 0015
Twist Rate	-8° per radius (linear)
Elastic Axis	25% chord
Chordwise CG	25% chord
Nominal Tip Speed	55 m/s (180.4 fps)
Hub Type	stiff-inplane hingeless
Precone	2.5°
Lock Number	6.12
Blade Mass	3.95 kg (8.71 lbm)
1st Mass Moment	0.374 kg-m (32.5 lbm-in)
Flap Inertia	0.161 kg-m sq (550.6 lbm-in sq)
Frequencies @ 430 rpm:	
1st Flap	1.30/rev
2nd Flap	4.09/rev
1st Torsion	4.74/rev

Carriage velocity changes were manually set prior to carriage "launch" down the track, and the return speed was also manually preset for each run. Data were recorded at approximately 330

Hz for each channel, and was allowed to fill one "page" of memory (64Kb) in an IBM-PC/AT prior to storage on a disk drive unit. Each data burst was approximately 4-5 seconds, and several data bursts would be collected during each carriage "run", which comprised a carriage launch, return, and capture/shutdown. Data runs are identified by number, with each segment collected during a carriage trip using a unique letter code. All runs followed a sequence of: beginning run zero point; rcal (resistor-calibrator) calibration data point; then a hover point, followed by as many climb and descent points as possible in the time it takes for each leg of the carriage trip. Data bursts that included obvious acceleration or deceleration transients were removed from the data sets summarized in this report's Appendix.

Data was reduced to coefficient form by first converting to engineering units, and then nondimensionalizing by tip speed, rotor disc area, and density. A paper presenting the initial results from this test (Reference 7, included here as an Appendix) used sea-level standard conditions for the density value; those data had not been corrected for the (rather uncomfortable!) lower density conditions during the experiment of approximately 93°F and 29.7 in Hg pressure. Such corrections would result in an approximate 7% increase in the nondimensional thrust and torque (power) coefficients over those shown in that reference. The correct nondimensional data are plotted along with the 1-sigma bounds on their variation for the 5 second data point in Figures 2 and 3, in order to provide additional information on the unsteadiness about the averaged value. Engineering units of force and moment for thrust and torque are accurate to within a half-percent of their full-scale value for the balance (30 lbf and 180 in-lbf, respectively). Thrust coefficient as a function of non-dimensional climb speed is in Figure 2, and the corresponding torque coefficient is given in Figure 3.

Test Results

As is evident from Figures 2 and 3, thrust immediately drops off from the hover value as vertical climb rate is increased, due to the reduction in effective blade section angle of attack, since the blades are operated at fixed collective pitch during the run. A similar reduction of thrust away from the hover value is evident in descent, although not as rapid, and is characteristic of the rotor entering a vortex ring state of operation. Rotor torque increases for increasing climb away from hover, and decreases during descent, since the velocity through the disc increases at a faster rate than the thrust decreases.

Simple Momentum Theory Analysis

A simple momentum analysis is useful in interpretation of the trends of thrust and torque for climb and descent away from hover operation. Following the approach of [8], if one equates the change in energy of the fluid inside a stream tube that includes the rotor disc at large distances above and below the disc plane, to the work done by the thrust on the flow through the disc area, the far-field downstream induced velocity can be shown to equal twice that induced at the rotor disc. Thus, in a vertical climb condition, the rotor thrust is:

$$T_{cl} = 2\rho A(v + V)v \tag{1}$$

where v is the induced velocity at the rotor disc, and V is the vertical climb velocity. Power expended to produce this thrust, neglecting any losses, is this thrust times the flow velocity through the disc:

$$P_{cl} = 2\rho A(v + V)^2 v \tag{2}$$

In hover, the climb velocity is zero, so these become:

$$T_h = 2\rho A v^2 \tag{3}$$

and

$$P_h = 2\rho A v^3 \tag{4}$$

Most expressions for climb power relative to hover power are based upon the assumption that hover thrust and climb thrust are equal, as they must be on a free-flying helicopter. However, since the test was conducted keeping blade pitch fixed, the climb thrust will be less than that in hover, and thus the ratio of climb power to hover power will include the ratio of thrust between the two cases according to:

$$\frac{P_{cl}}{P_h} = \frac{(v+V)^2 v}{v_h^3} = \left(\frac{T_{cl}}{T_h}\right)\left(\frac{v+V}{v_h}\right) \tag{5}$$

The expression for the ratio of climb to hover disc velocities may be computed as a function of the thrust ratio, by solving a quadratic equation that results from finding the ratio of climb to hover thrust:

$$\left(\frac{T_{cl}}{T_h}\right) = \left(\frac{v+V}{v_h}\right)\left(\frac{v}{v_h}\right) = \left(\frac{v}{v_h}\right)^2 + \left[\frac{V}{v_h}\right]\left(\frac{v}{v_h}\right) \tag{6}$$

Hence, given the climb velocity, hover thrust, and climb thrust, one may compute the ratio of climb power to hover power, and compare this result to the actual power ratio computed from the test data. Figure 4 shows this comparison, and indicates that momentum theory overpredicts the power required to climb, when both hover power is known and all incremental power is assumed to be induced. Correspondingly, momentum theory overpredicts the power reduction realized during moderate descent velocities, although it should be noted that the inherent assumptions about the wake around the rotor disc break down in this regime. This discrepancy between the test data and simple momentum theory are further presented in Figure 5, where the actual climb power ratio is plotted against the predicted ratio, again using measured thrust values to compute the momentum inflow values. Differences between the data points and the solid line indicate divergence of the data away from a purely momentum-based analysis. These results are consistent with those presented by Harris in [2].

Other Theories

Further analysis of these data, including comparisons with both fixed and free-wake analysis models, are given in the Appendix, which consists of a reprint of Reference 7, cited below.

References

1. Crawford, C.C., Jr., "Rotorcraft Analytical Improvement Needed to Reduce Developmental Risk - The 1989 Alexander Nikolsky Lecture," Journal of the American Helicopter Society, Vol. 35, n.1, January 1990.

2. Harris, F. D., "Rotary Wing Aerodynamics - Historical Perspective and Important Issues," AHS National Specialists' Meeting on Aerodynamics and Aeroacoustics, Fort Worth, Texas, 1987.

3. Moffitt, R. C., and Sheehy, T. W., "Prediction of Helicopter Rotor Performance in Vertical Climb and Sideward Flight," Proc. 33rd AHS Annual Forum, Washington, D.C., May 1977.

4. McKillip, R. M., Jr., "Experimental Studies in System Identification of Helicopter Rotor Dynamics", Vertica, Vol. 12, n. 4, 1988.

5. Curtiss, H. C., Jr., Erdman, W. and Sun, M., "Ground Effect Aerodynamics," Vertica, Vol. 11., n. 1/2, 1987.

6. Putman, W. F. and Traybar, J. J., "An Experimental Investigation of Compound Helicopter Aerodynamics in Level and Descending Forward Flight and in Ground Proximity", USAAMRDL TR 71-19, July 1971.

7. Felker, F., and McKillip, R., "Comparisons of Predicted and Measured Rotor Performance in Vertical Climb and Descent," Proc. 50th AHS Annual Forum, Washington, D.C., May 1994.

8. Johnson, W. Helicopter Theory. Princeton University Press, Princeton, N.J., 1980.

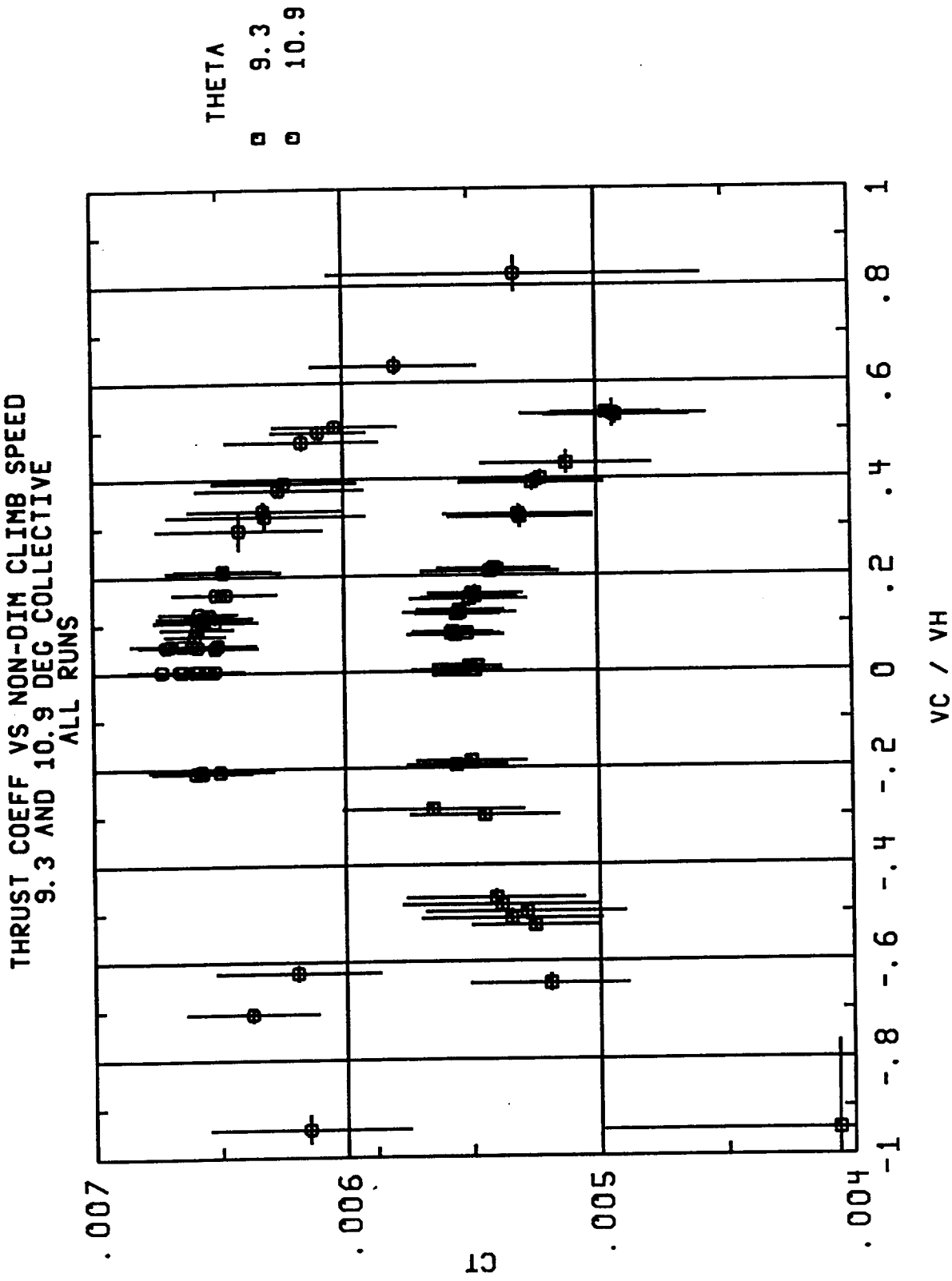
THRUST COEFF VS NON-DIM CLIMB SPEED
9.3 AND 10.9 DEG COLLECTIVE
ALL RUNS
THETA
9.3
10.9
CT
.007
.006
.005
.004
-1
-.8
-.6
-.4
-.2
0
.2
.4
.6
.8
1
VC / VH

Figure 2

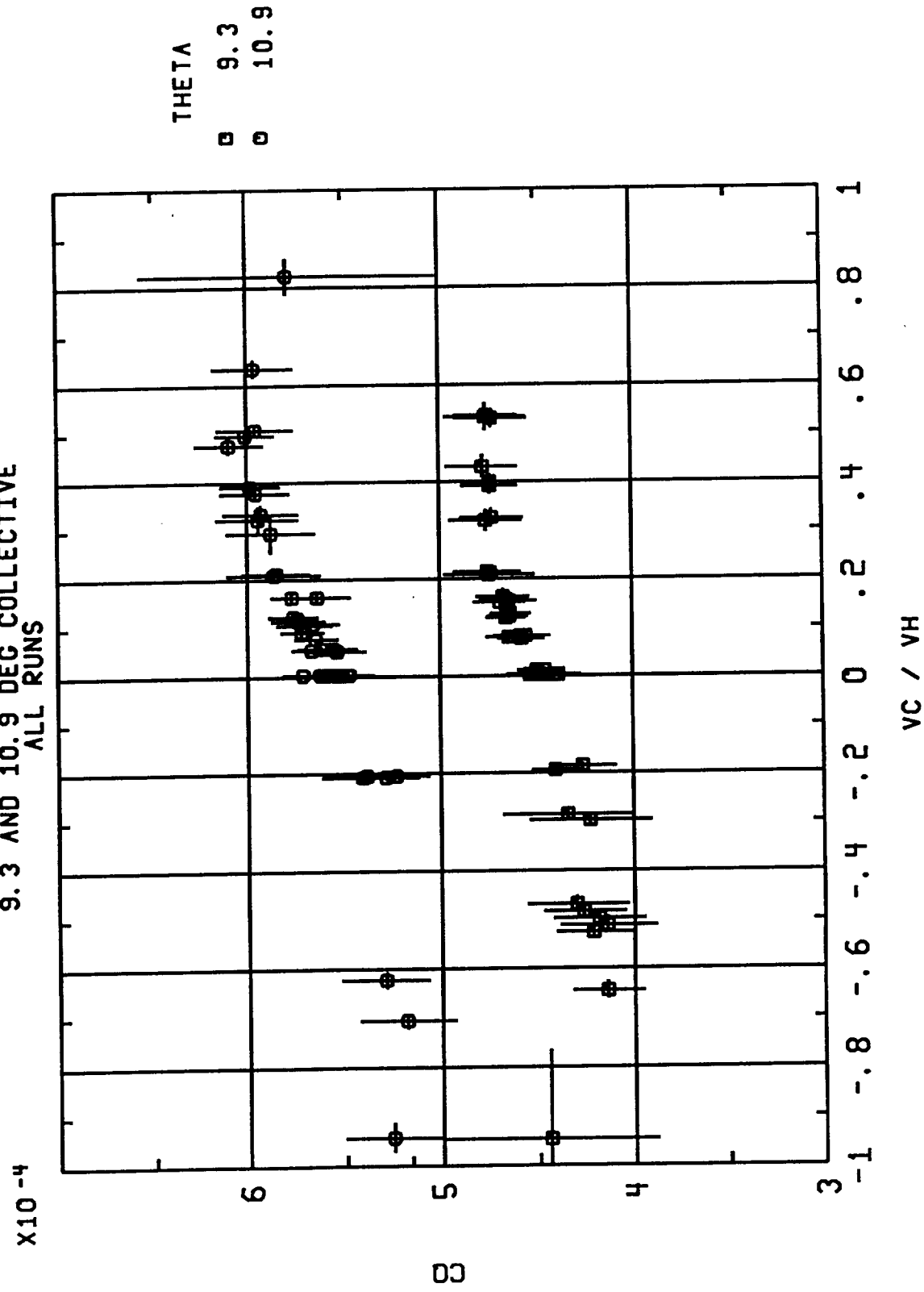
TORQUE COEFF VS NON-DIM CLIMB SPEED
9.3 AND 10.9 DEC COLLECTIVE
ALL RUNS
THETA
9.3
10.9
X10-4
CQ
6
5
4
3
-1
-.8
-.6
-.4
-.2
0
.2
.4
.6
.8
1
VC / VH

Figure 3

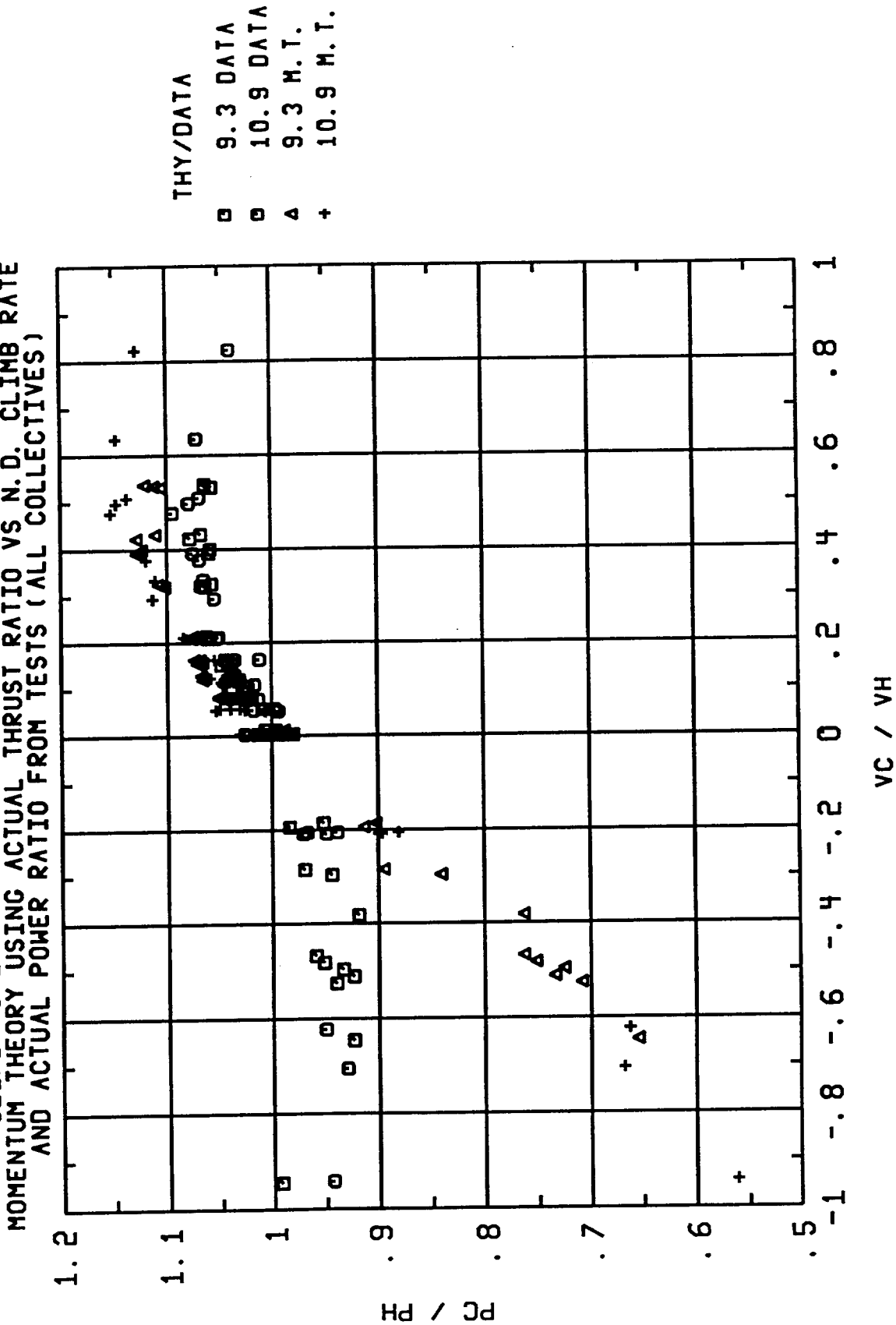
CLIMB POWER RATIO CORRECTED FOR VARIABLE THRUST
MOMENTUM THEORY USING ACTUAL THRUST RATIO VS N.D. CLIMB RATE
AND ACTUAL POWER RATIO FROM TESTS (ALL COLLECTIVES)
THY/DATA
9.3 DATA
10.9 DATA
9.3 M.T.
10.9 M.T.
PC / PH
VC / VH
1.2
1.1
1
.9
.8
.7
.6
.5
-1
-.8
-.6
-.4
-.2
0
.2
.4
.6
.8
1

Figure 4

Figure 5

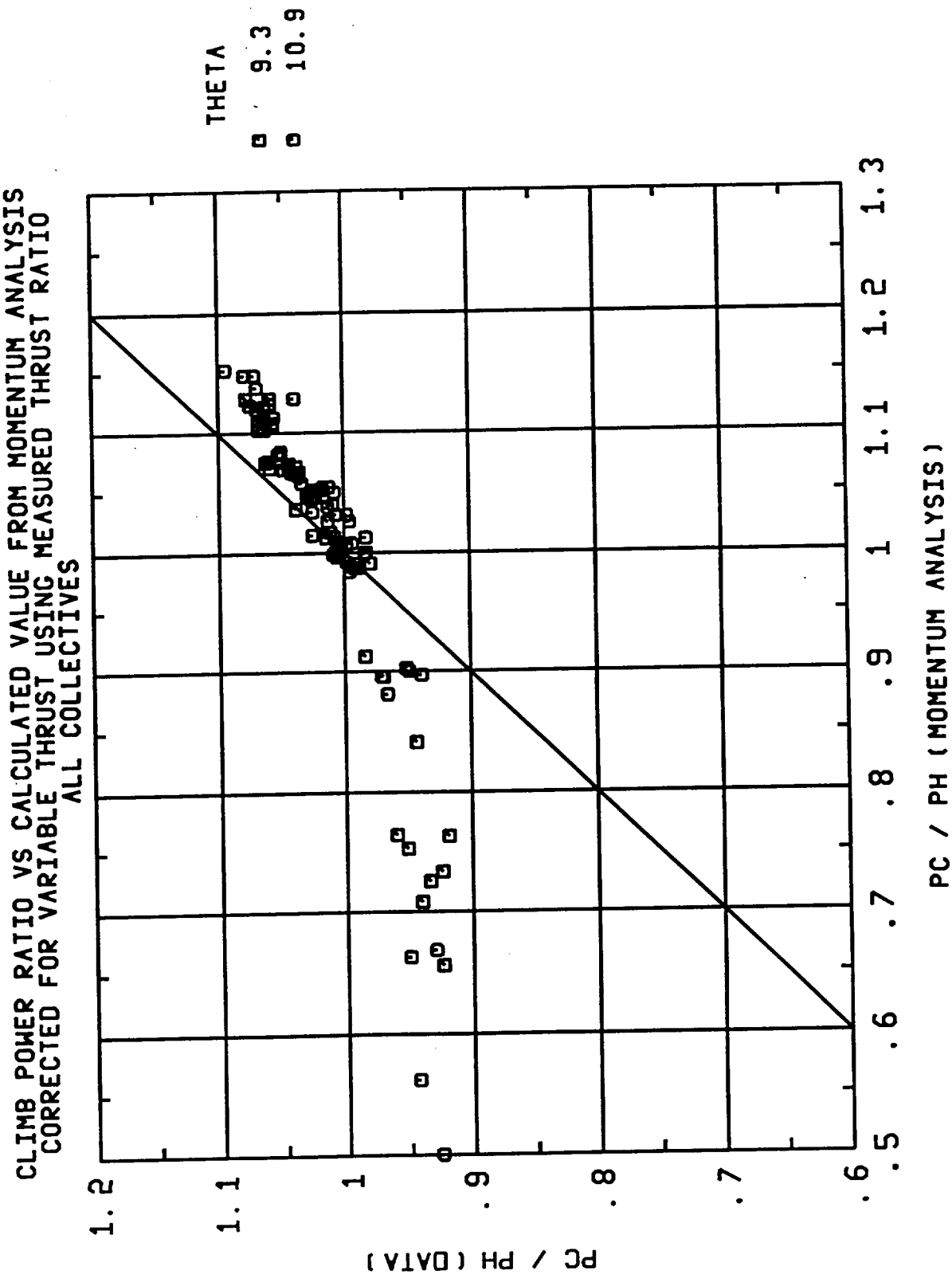
CLIMB POWER RATIO VS CALCULATED VALUE FROM MOMENTUM ANALYSIS
CORRECTED FOR VARIABLE THRUST USING MEASURED THRUST RATIO
ALL COLLECTIVES
THETA
9.3
10.9
PC / PH (DATA)
PC / PH (MOMENTUM ANALYSIS)
1.2
1.1
1
.9
.8
.7
.6
.5
.6
.7
.8
.9
1
1.1
1.2
1.3

COMPARISONS OF PREDICTED AND MEASURED ROTOR PERFORMANCE IN VERTICAL CLIMB AND DESCENT

Fort F. Felker
Staff Scientist
NASA Ames Research Center
Moffett Field, California

Robert M. McKillip
Senior Associate
Continuum Dynamics, Inc.
Princeton, New Jersey

Abstract

An experimental and theoretical investigation was conducted to provide accurate measurements of rotor performance in vertical climb and descent, and to assess the ability of various analyses to predict that performance. The experiment was performed in the Princeton Long Track, which effectively eliminated the uncertainties in rotor thrust and axial flight speed which have plagued earlier measurements of axial flight performance in wind tunnel and flight tests. Three analytical approaches were examined: momentum theory, a prescribed wake analysis, and a free-wake analysis. This paper presents the experimental data, and assesses the accuracy of the various analytical approaches.

Nomenclature

C_P	rotor power coefficient
C_T	rotor thrust coefficient
R	rotor radius, m
V_c	climb velocity, m/s
V_h	ideal induced velocity in hover, m/s, $V_h = \Omega R\sqrt{C_T/2}$
θ	rotor collective pitch at 3/4 radius, deg
Ω	rotor rotational speed, rad/s

Introduction

The accurate prediction of rotorcraft vertical climb and descent performance remains a difficult problem in rotorcraft aerodynamics. It has been reported that a widely-used vertical climb performance analysis method (momentum theory) can overpredict the power increment required to climb by 50% or more (Ref. 1).

The lack of an accurate analysis creates a severe difficulty during the development of a new helicopter. For example, the U.S. Army specifies a minimum level of vertical climb performance that is acceptable, and imposes severe penalties if a newly-developed helicopter cannot meet the specification. Since the analysis is not accurate, it is impossible to know whether or not a proposed design can meet the specification until testing of the prototype helicopter is underway. At that point in the development cycle, design changes to meet the specification are very costly. The situation was succinctly summed up by Harris (Ref. 1): "It is a very serious matter when a performance requirement can be specified by the user and no real aerodynamic design technology exists" (emphasis by Harris).

Adding to the difficulty of vertical climb performance prediction is the lack of high-quality experimental data. Many of the experimental investigations of rotor axial flight performance have focused on the vertical descent case, with descent rates up to that required for autorotation (e.g. Ref. 2). These investigations were motivated by concerns about helicopter vertical descent rates in the event of engine failure. Of the experimental data on vertical climb performance, the flight test data (see Ref. 1 for a useful compilation) are compromised by uncertainties in the actual rotor thrust, and the difficulty of maintaining a truly vertical flight path. The available wind tunnel data (e.g. Refs. 3-4) are compromised by uncertainties in the axial velocity and wind tunnel wall effects.*

The principal analytical method for vertical climb and descent performance predictions has been momentum theory (Ref. 6 provides a typical analysis). Because of the well-known limitations of momentum theory, Moffitt and Sheehy (Ref. 7), and Kocurek and Berkowitz (Ref. 8) developed modified prescribed-wake methods for use in vertical climb. The results shown in Ref. 7 indicated that the modified prescribed-wake method was substantially more accurate than momentum theory for vertical climb performance. A free-wake analysis for axial-flight performance developed by Quackenbush, et al (Refs. 9-10)

Presented at the American Helicopter Society 50th Annual Forum, Washington, DC, May 11-13, 1994.

* The vertical climb performance data in Ref. 4 were not corrected for wind tunnel wall effects. Using the wall correction methodology of Glauert (Ref. 5), the equivalent climb velocity for the data of Ref. 4 becomes $V_c/V_h = 0.455 \pm 0.010$, instead of the reported value of 0.545 ± 0.010.

has also demonstrated improved results compared to momentum theory in vertical climb (Ref. 11).

This paper describes a combined theoretical and experimental investigation into rotorcraft performance in vertical climb and descent. High-quality performance data were acquired in the Princeton Long Track. This facility allowed for the model to be mounted on an accurate balance system and moved through still air in a controlled environment. This approach eliminated the uncertainties in rotor thrust and axial flight speed common in flight and wind tunnel tests.

The performance of this rotor was predicted using a range of analytical approaches. The rotor inflow was calculated using momentum theory, a prescribed-wake method, and a free-wake analysis. Comparisons between the predicted and measured performance are used to establish the accuracy of the different analytical methods.

Experimental Results

The test was conducted in the Princeton Long Track* (Fig. 1). The Long Track allowed for models to be moved through still air along the length of the 225 m building. The model speed could be precisely controlled, and the 10 m x 10 m cross section of the facility eliminated the need for wall corrections for the 2-3 m diameter rotors which were typically tested. The rotor was installed on the model-carriage balance system, which measured the rotor performance. This experimental approach eliminated the uncertainties in rotor thrust inherent in flight tests, and the uncertainties in tunnel speed and wall corrections inherent in wind tunnel tests of axial flight performance.

Figure 1. Aerial photograph of Princeton's Long Track.

* This was the final test in the Long Track before its demolition in the summer of 1992. Princeton's Long Track was the site of many fundamental advances in rotorcraft aerodynamics.

The model rotor had 4 blades and a diameter of 2.44 m. A summary of the important rotor system parameters is provided in Table 1. The model rotor was originally designed for Froude-scale testing, and was therefore operated at a reduced tip speed. The rotor system was a stiff-inplane hingeless design, and collective pitch was mechanically adjusted between runs. Cyclic pitch was set to zero. The blade pitch control system eliminated any possibility of the blade root pitch varying during a data acquisition run, or with rotor thrust changes. The rotor axis was horizontal, so that an axial-flight condition was maintained as the rotor was moved down the Long Track on the model carriage system. A photograph of the model rotor installed in the Long Track is provided as Fig. 2.

Table 1. Summary of Rotor System Parameters

Number of Blades	4
Radius	2.44 m
Root Cutout	10% radius
Blade Chord	0.0635 m
Solidity	0.0663
Airfoil	NACA 0015
Twist Rate	-8 deg per radius
Nominal Tip Speed	55 m/s
Hub Type	stiff-inplane hingeless
Precone	3 deg
Lock Number	6.12
Flap Inertia	0.161 kg-m^2
1st Flap mode	1.30/rev
1st Torsion mode	4.74/rev

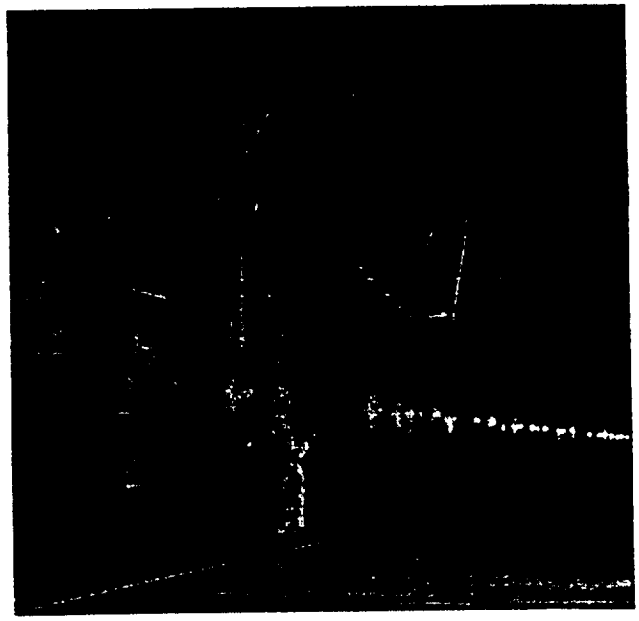

Figure 2. Model rotor installed in Princeton Long Track.

Data were acquired at two collective pitch settings, 9.3 deg and 10.9 deg. Figure 3 shows the effect of axial flight speed on the rotor thrust coefficient, and Fig. 4 shows the effect of axial flight speed on rotor power coefficient. A complete tabulation of the data is provided in the Appendix.

In hover, the average rotor thrust coefficients were 0.00514 and 0.00612, and the average rotor power coefficients were 0.000422 and 0.000523, at the collective pitches of 9.3 deg and 10.9 deg, respectively. The closed test environment unavoidably introduced some unsteadiness into the hover performance measurements (see Ref. 12 for a discussion of unsteadiness in indoor hover performance tests). This unsteadiness was reduced as the climb velocity was increased.

Because the data were acquired at fixed collective pitch, increasing the climb velocity reduces the rotor blade sectional angles of attack, which reduces the rotor thrust coefficient (Fig. 3). In spite of the reduced thrust, the rotor power initially increases with increasing climb velocity (Fig. 4). This increase in power is caused by the work of the thrust moving through the air. As the climb velocity is increased further, the reduction in rotor thrust is eventually large enough to cause a corresponding reduction in rotor power.

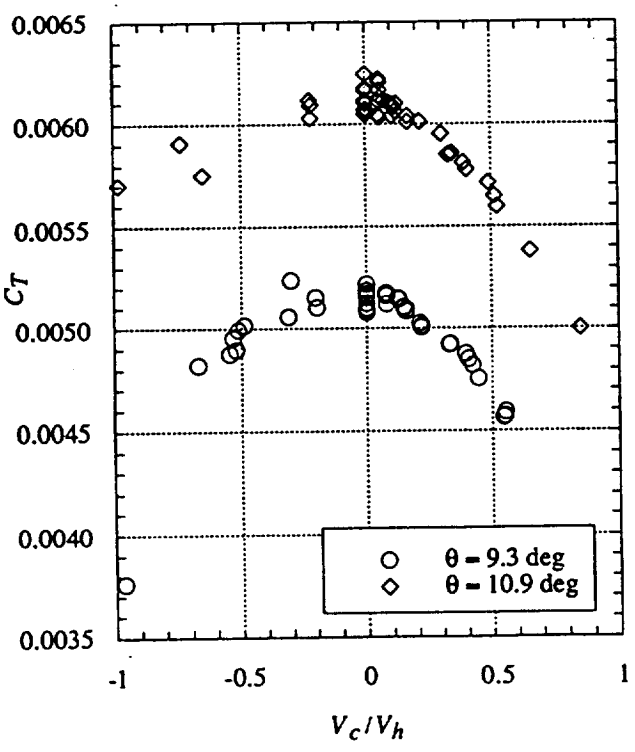

Figure 3. Effect of vertical climb velocity on measured rotor thrust coefficient.

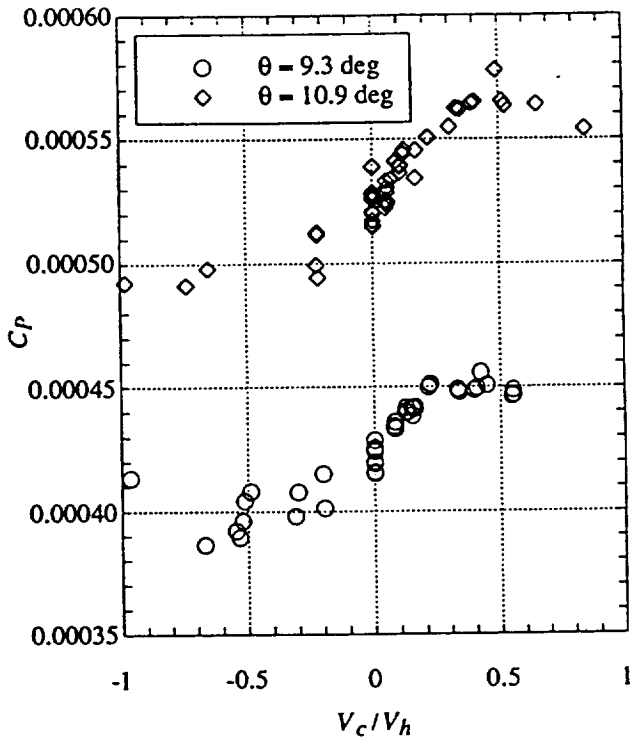

Figure 4. Effect of vertical climb velocity on measured rotor power coefficient.

It might be expected that axial descent would produce the opposite result as axial climb, with increasing sectional angles of attack and increasing rotor thrust coefficients. However, as Fig. 3 shows, this does not occur. The rotor very quickly enters the vortex ring state, which fundamentally alters the flow field around the rotor (see Ref. 13 for a discussion of the aerodynamics of the vortex ring state). The increased scatter in the rotor power coefficient in vertical descent is characteristic of the unsteady vortex ring state.

Analysis Results

The rotor performance in axial flight was predicted using three methods for determining the rotor inflow. The inflow was computed using uniform inflow (from momentum theory), a prescribed-wake method, and a free-wake method.

Uniform inflow methods can provide accurate predictions of hover performance when correctly tuned (Refs. 14-15). However, the predicted blade loading distributions obtained with uniform inflow methods are incorrect, and are not suitable for detailed blade design work. Prescribed-wake methods were developed to overcome this limitation, and extensions of these methods to vertical climb are described in Refs. 7 and 8. Prescribed-wake analyses are

based on fairings of experimental wake geometry data. The possibility always exists that the wake of a rotor substantially different than those used to generate the experimental data base will not be well-predicted using the prescribed-wake analyses. Free-wake methods predict the wake geometry without resorting to empiricisms, and can provide the most general and realistic solutions.

The uniform inflow and prescribed-wake methods were evaluated using CAMRAD/JA (Ref. 16). The free-wake method was evaluated using EHPIC (Refs. 9-10). Both of these analyses required specification of airfoil profile drag through the use of airfoil tables. The tip Reynolds number of the model rotor was only 240,000. Airfoil test data at this low Reynolds number were obtained from Ref. 17, and the airfoil table constructed with this data was used for both analyses. No unusual tuning of the analyses was done to improve the correlation with test data. Thus, the results presented here should be representative of what could be obtained for a new design, prior to the acquisition of test data.

Uniform Inflow

Following typical practice (Refs. 14-15), the uniform inflow velocity was increased by 10 percent relative to the ideal momentum theory value to account for non-ideal effects. The rotor wake extended for 5 revolutions, which was the maximum allowed by CAMRAD/JA. Other input parameters were set at values recommended in the code's documentation.

For the hover case, the blade pitch was trimmed to match the average experimental thrust coefficient. The predicted root pitch agreed with the experimental value to within 0.2 deg. The predicted power in hover was 1.4 and 1.7 percent higher than the average measured in the experiment for the low and high pitch cases, respectively. This degree of correlation in collective pitch and power is very good for a uniform inflow analysis.

To follow the experimental data acquisition method, the analysis was run with varying climb speeds while the collective was held fixed at the value required to match the average thrust coefficient in hover. A comparison of the predicted and measured thrust coefficients is shown in Fig. 5, and a comparison of the predicted and measured power coefficients is shown in Fig. 6.

Both the thrust and the power were underpredicted by the analysis in vertical climb. The errors in thrust and power were about 10 percent at nondimensional climb velocities of 0.5. In descent, the results do not agree even qualitatively with the test data, confirming that momentum theory provides a poor representation of rotor aerodynamics in vertical descent.

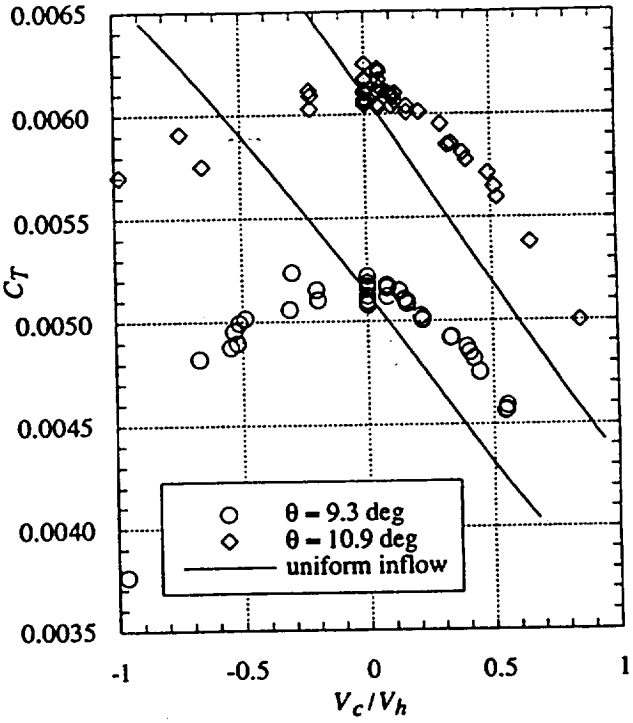

Figure 5. Comparison of predicted and measured rotor thrust with uniform inflow and fixed collective.

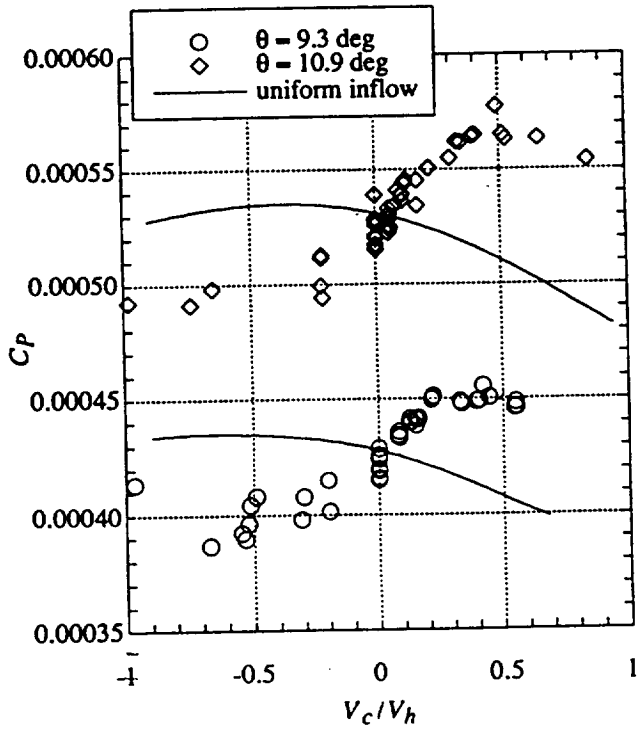

Figure 6. Comparison of predicted and measured rotor power with uniform inflow and fixed collective.

In Fig. 5, the experimental data show that for climb velocities near zero the climb velocity has essentially no effect on the thrust coefficient (zero slope of C_T vs. V_c/V_h at zero climb velocity). The uniform inflow thrust calculations exhibit a fairly constant slope over the entire range of climb velocities. This error in slope of C_T vs. V_c/V_h at zero climb velocity causes the differences in predicted and measured thrust coefficient for positive climb velocities. Note that the experimental data do match the slope of the predictions for nondimensional climb velocities greater than 0.5.

Figure 6 shows that the rotor power is underpredicted in climb. However, the errors in the predicted power were largely a consequence of the errors in the predicted thrust. To demonstrate this, the analysis was run with the collective pitch trimmed to match the observed thrust coefficient (curve fits of the experimental C_T vs. V_c/V_h data were used to determine the trim thrust coefficient). Also, for design purposes the rotor power at a specified thrust is of greater interest than the trends of thrust and power at fixed collective. The collective pitch changes (relative to the fixed-pitch case) required to match the experimental thrust coefficient were less than 0.8 deg.

A comparison between the predicted and measured power when matching the thrust coefficient is shown in Fig. 7. Here, the agreement between theory and data is excellent. This shows that a method using uniform inflow/momentum theory can provide accurate predictions of rotor power in vertical climb if the collective pitch is trimmed to obtain the required thrust (this is the normal operational mode of a performance analysis).

The rotor power in vertical descent was also predicted with the measured thrust coefficient matched by the analysis. Unlike the vertical climb case, this effort was not successful for vertical descent. The predicted power was about 10 percent less than the measured power at a nondimensional vertical descent velocity of $V_c/V_h = -0.5$.

Prescribed Wake

The prescribed wake geometry was computed using the velocity-coupled prescribed-wake relations given in Ref. 8,* and manually input into CAMRAD/JA. No information was provided in Ref. 8 on how the inboard vortex sheet geometry depends on the climb velocity. For this investigation the effect of vertical climb on the inboard sheet geometry was modeled by increasing the axial descent rates of the sheet by the climb advance ratio $V_c/\Omega R$. Typical

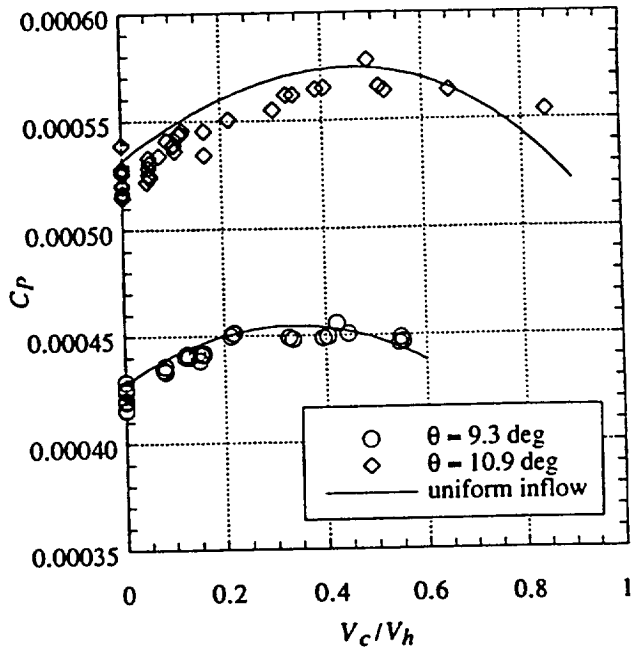

Figure 7. Comparison of predicted and measured rotor power with uniform inflow. Collective pitch varied to match measured thrust.

practice for CAMRAD/JA is to reduce the tip vortex far wake axial descent rate in hover by approximately 10% to compensate for the truncation of the wake model after 5 revolutions (Refs. 14-15). However, this empirical factor was not used here because of uncertainties in whether it was appropriate in vertical climb, and because use of such a factor would be inconsistent with the prescribed-wake model of Ref. 8. Since the wake is truncated in CAMRAD/JA, the resulting performance predictions should be optimistic (underprediction of induced power).

In hover, the blade pitch was trimmed to match the experimental thrust coefficient. The root pitch was underpredicted by 0.2 and 0.4 deg for the low and high pitch cases, respectively. The predicted power in hover was 3.6 and 3.1 percent lower than the average measured in the experiment for the low and high pitch cases. The good correlation between theory and test data for both power and collective pitch in hover provides confidence that the velocity-coupled prescribed-wake method has been correctly implemented. Inclusion of a more extensive wake than the 5 turns allowed by CAMRAD/JA would increase the induced velocity at the rotor. The increased induced velocity would increase the collective pitch for a given thrust coefficient, and increase the induced power, improving correlation with the test data.

* In Ref. 8 the equations for the mean wake settling rate (eqns. 15 and 18) contain a typographical error. The denominator in these equations should contain the term 4π instead of 2π as shown.

Despite persistent efforts to apply the velocity-coupled prescribed-wake model to vertical climb, no converged solutions were obtained. Successive iterations with the model monotonically increased the tip vortex axial descent rates beyond physically possible values. Many different climb rates, initial conditions, and convergence strategies were tried without success. Although the possibility of implementation errors can never be completely ruled out, the success of the method in hover, and a careful checking and rechecking of the implementation lend confidence that the model was implemented as described in Ref. 8. From these results, along with the success of the uniform inflow and free-wake analysis (see next section and Ref. 11), we conclude that the prescribed-wake method of Ref. 8 is insufficiently robust for vertical climb performance predictions.

Free Wake

The free-wake analysis EHPIC imposes a slope boundary condition on all vortices trailed from the rotor blade. At the blade trailing edge the vortices are constrained to be parallel to the blade chord line. This boundary condition is appropriate and consistent with the Kutta condition for inboard blade stations. However, this boundary condition is not appropriate for the blade tip, where three-dimensional effects invalidate the Kutta condition. This boundary condition is discussed further in Ref. 11, and examples are provided which show how it leads to errors in the predicted wake geometry prior to first blade passage. This boundary condition also prevents the tip vortex geometry near the rotor blade from being affected by vertical climb velocities.

For these reasons a new tip vortex boundary condition was implemented. The slope of the tip vortex at the blade was constrained to be equal to the climb advance ratio $V_c/\Omega R$ (a better choice would be to set the slope equal to the sum of the climb velocity and the ideal induced velocity, divided by the tip speed). The boundary condition for the inboard vortices was not altered. This change provided slightly more accurate predictions of rotor performance in vertical climb. The comparisons of predicted and measured tip vortex geometry in hover shown in Ref. 11 were re-run with the new boundary condition, and the new results show improved predictions of tip vortex geometry prior to first blade passage.

In hover the blade collective pitch angle was trimmed to match the average measured thrust coefficient. The predicted power was 2.6 and 3.4 percent higher than the average measured power for the low and high pitch cases, respectively. The predicted root pitch agreed with the experimental data to within 0.3 deg. These results are typical of the accuracy which is normally achieved with this analysis (Ref. 11).

To again follow the experimental data acquisition method, the free-wake analysis was run with varying climb speeds while the collective was held fixed at the value required to match the thrust coefficient in hover. A comparison of the predicted and measured thrust coefficients is shown in Fig. 8, and a comparison of the predicted and measured power coefficients is shown in Fig. 9.

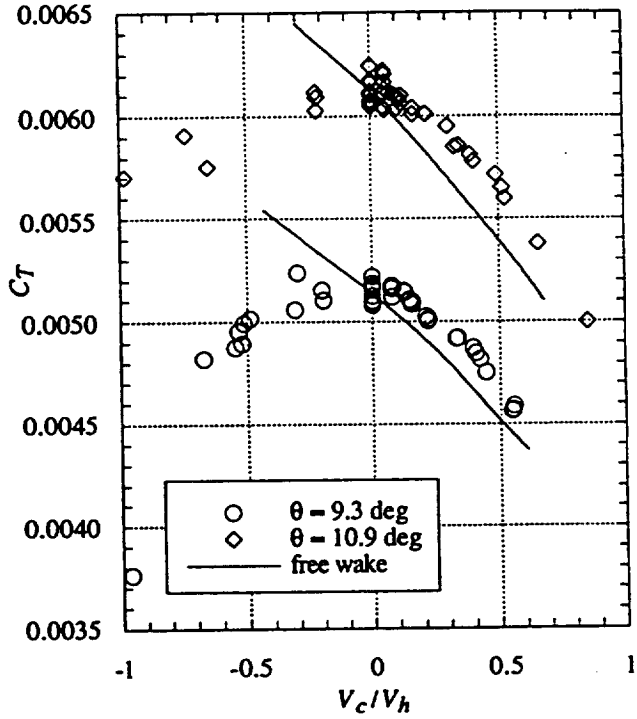

Figure 8. Comparison of predicted and measured rotor thrust with free wake and fixed collective.

Like the uniform inflow analysis, the free-wake analysis underpredicted the rotor thrust and power in vertical climb. However, the errors in thrust and power (approximately 5 percent at a nondimensional climb velocity of 0.5) were only about one-half as large as the errors obtained with the uniform inflow analysis. Like the uniform inflow analysis, the free-wake analysis incorrectly predicts a non-zero slope for the rotor thrust vs. climb velocity curve at zero climb velocity.

The prediction of thrust and power in vertical descent by the free-wake analysis was poor, but was somewhat better than the uniform inflow analysis. However, the free-wake analysis would not converge for nondimensional descent velocities in excess of -0.45. This suggests that a steady flow solution may not exist at these descent rates. This would be consistent with the unsteady flow observed in experiments when rotors are operated in the vertical descent vortex ring state.

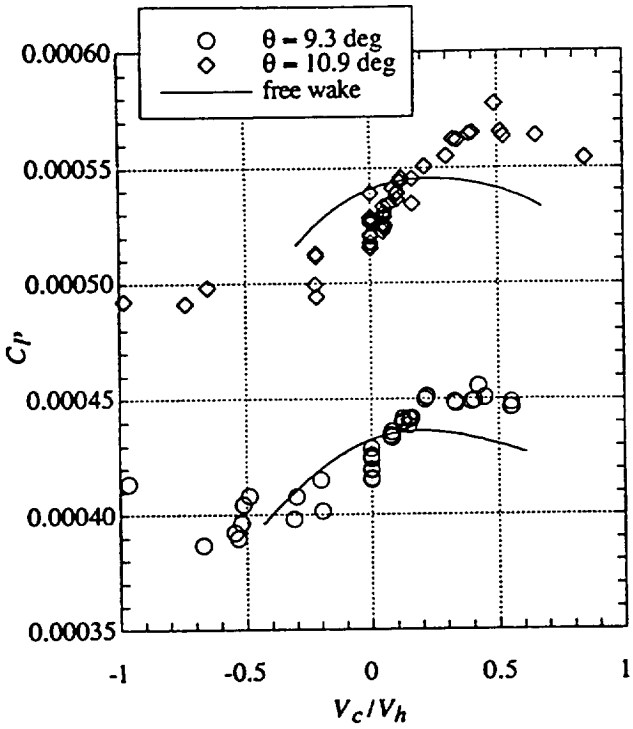

Figure 9. Comparison of predicted and measured rotor power with free wake and fixed collective.

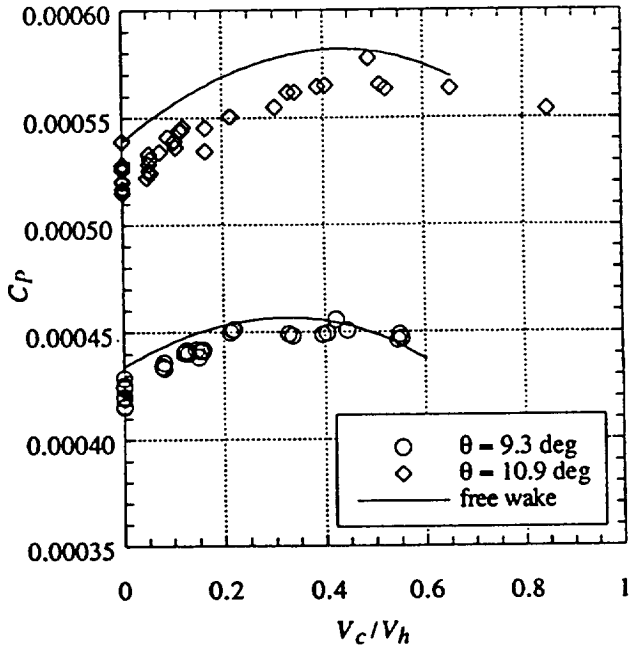

Figure 10. Comparison of predicted and measured rotor power with free wake. Collective pitch varied to match measured thrust.

For design purposes the rotor power at a specified thrust is of greater interest than the trends of thrust and power at fixed collective. The free-wake analysis was therefore run with the collective pitch trimmed to match the measured thrust coefficient. The changes in collective pitch required to match the thrust were less than 0.5 deg.

Figure 10 shows a comparison between the predicted and measured power when matching thrust. Excellent results were obtained for the low pitch case. For the high pitch case the power was overpredicted by a fairly constant factor for nondimensional climb velocities up to 0.5. This constant error factor is consistent with the 3.4 percent overprediction of power obtained in hover, suggesting a possible overprediction of profile power for the high pitch case. The results obtained with the free-wake analysis were not quite as accurate as the uniform inflow results when the thrust coefficient was matched.

The rotor power in vertical descent was also predicted with the measured thrust coefficient matched by the analysis. Again, poor results were obtained, with the predicted power over 15 percent less than the measured power at a nondimensional vertical descent velocity of V_c/V_h = -0.45.

Conclusions

A combined experimental and theoretical investigation of rotor performance in vertical climb and descent has been completed. The test data are free of the uncertainties in vertical climb velocity, rotor thrust, and wall interference effects which have plagued earlier measurements. Specific conclusions from this research are:

1. Rotor thrust was essentially unchanged by small vertical climb or descent velocities (magnitude of V_c/V_h less than 0.1).

2. At fixed collective pitch, momentum theory underpredicted the rotor thrust and power in vertical climb. The errors in thrust and power were about 10% at a nondimensional climb velocity of 0.5.

3. The free-wake analysis also underpredicted the rotor thrust and power in vertical climb at fixed collective, but the errors were about one half as large as those obtained with momentum theory.

4. When collective pitch was allowed to vary to obtain the desired thrust, both momentum theory and the free-wake analysis provided accurate power predictions. For this case, the momentum theory results were slightly more accurate than the free-wake analysis results.

5. The velocity-coupled prescribed-wake method provided accurate results in hover. However, this method is insufficiently robust to provide results for the vertical climb case.

6. None of the analytical methods were able to provide satisfactory predictions in vertical descent.

Acknowledgment

The authors gratefully acknowledge the assistance of W. Putnam with the test in the Long Track, and the assistance of M. Hagen with the free-wake calculations.

References

1. Harris, F. D., "Rotary Wing Aerodynamics: Historical Perspectives and Important Issues," American Helicopter Society Specialists' Meeting on Aerodynamics and Aeroacoustics, Fort Worth, Texas, February 1987.

2. Castles, W., and Gray, R. B., "Empirical Relation Between Induced Velocity, Thrust, and Rate of Descent of a Helicopter Rotor as Determined by Wind Tunnel Tests on Four Model Rotors," NACA TN-2474, October 1951.

3. Yeager, W. T., Young, W. H., and Mantay, W. R., "A Wind Tunnel Investigation of Parameters Affecting Helicopter Directional Control at Low Speeds in Ground Effect," NASA TN D-7694, November 1974.

4. Felker, F. F., "Results from a Test of a 2/3-Scale V-22 Rotor and Wing in the 40- by 80-Foot Wind Tunnel," American Helicopter Society 47th Annual Forum, Phoenix, Arizona, May 1991.

5. Glauert, H., The Elements of Aerofoil and Airscrew Theory, Cambridge University Press, New York, 1947, pp. 222-226.

6. Prouty, R. W., Helicopter Performance, Stability, and Control, PWS Engineering, Boston, 1986, pp. 97-101.

7. Moffitt, R. C., and Sheehy, T. W., "Prediction of Helicopter Performance in Vertical Climb and Sideward Flight," American Helicopter Society 33rd Annual Forum, Washington, D.C., May 1977.

8. Kocurek, J. D., and Berkowitz, L. F., "Velocity Coupling - A New Concept for Hover and Axial Flow Wake Analysis and Design," AGARD CP-334, September 1982.

9. Quackenbush, T. R., Bliss, D. B., Wachspress, D. A., and Ong, C. C., "Free Wake Analysis of Hover Performance Using a New Influence Coefficient Method," NASA CR 4309, July 1990.

10. Quackenbush, T. R., Boschitsch, A. H., Wachspress, D. A., and Chua, K., "Rotor Design Optimization Using a Free Wake Analysis," NASA CR 177612, April 1993.

11. Felker, F. F., Quackenbush, T. R., Bliss, D. B., and Light, J. S., "Comparisons of Predicted and Measured Rotor Performance in Hover Using a New Free-Wake Analysis," *Vertica*, Vol. 14, (3), December 1990.

12. Piziali, R. A., and Felker, F. F., "Reduction of Unsteady Recirculation in Hovering Model Helicopter Rotor Testing," *Journal of the American Helicopter Society*, Vol. 32, (1), January 1987.

13. Johnson, W., Helicopter Theory, Princeton University Press, New Jersey, 1980, pp. 98-105.

14. Reddy, K. R., and Gilbert, N. E., "Comparison with Flight Data of Hover Performance Using Various Rotor Wake Models," Thirteenth European Rotorcraft Forum, Arles, France, September 1987.

15. Felker, F. F., "Accuracy of Tilt Rotor Hover Performance Predictions," NASA TM 104023, June 1993.

16. Johnson, W., "A Comprehensive Analytical Model of Rotorcraft Aerodynamics and Dynamics," NASA TM-81182, June 1980.

17. Knight, M., and Hefner, R. A., "Static Thrust Analysis of the Lifting Airscrew," NACA TN-626, December 1937.

Appendix: Tabulated Experimental Data

Run-Pt.	θ, deg	V_c/V_h	C_T	C_P
2-1	9.3	0.000	0.00508	0.000420
2-2	9.3	0.150	0.00510	0.000438
2-3	9.3	0.146	0.00511	0.000442
2-4	9.3	0.152	0.00508	0.000441
2-5	9.3	0.159	0.00509	0.000441
2-6	9.3	0.158	0.00508	0.000442
3-1	9.3	0.000	0.00510	0.000426
3-2	9.3	0.422	0.00482	0.000456
3-3	9.3	0.405	0.00485	0.000449
3-4	9.3	0.395	0.00487	0.000449
3-5	9.3	-0.512	0.00499	0.000404
4-1	9.3	0.000	0.00509	0.000419
5-1	9.3	0.000	0.00510	0.000415
5-2	9.3	0.335	0.00492	0.000448
5-3	9.3	0.328	0.00492	0.000449
5-4	9.3	-0.205	0.00515	0.000415
5-5	9.3	-0.197	0.00511	0.000401
6-1	9.3	0.000	0.00512	0.000416
6-2	9.3	0.125	0.00514	0.000442
6-3	9.3	0.122	0.00515	0.000440
6-4	9.3	0.130	0.00514	0.000440
6-5	9.3	-0.311	0.00506	0.000398
6-6	9.3	-0.302	0.00524	0.000408
7-1	9.3	0.000	0.00517	0.000429
7-2	9.3	0.213	0.00503	0.000450
7-3	9.3	0.217	0.00500	0.000451
7-4	9.3	0.220	0.00501	0.000451
7-5	9.3	-0.488	0.00502	0.000408
8-1	9.3	0.000	0.00516	0.000424
8-2	9.3	0.080	0.00512	0.000436
8-3	9.3	0.081	0.00517	0.000436
8-4	9.3	0.081	0.00517	0.000433
8-5	9.3	0.077	0.00516	0.000434
8-6	9.3	0.078	0.00518	0.000434
8-7	9.3	-0.521	0.00490	0.000396
9-1	9.3	0.000	0.00519	0.000424
9-2	9.3	0.444	0.00475	0.000451
9-4	9.3	-0.547	0.00488	0.000392
9-5	9.3	-0.533	0.00495	0.000390
10-1	9.3	0.000	0.00522	0.000425
10-2	9.3	0.546	0.00456	0.000446
10-3	9.3	0.553	0.00459	0.000447
10-4	9.3	-0.967	0.00376	0.000414
11-2	9.3	0.550	0.00457	0.000449
11-3	9.3	-0.672	0.00482	0.000387

Run-Pt.	θ, deg	V_c/V_h	C_T	C_P
12-1	10.9	0.000	0.00618	0.000539
12-2	10.9	0.491	0.00571	0.000577
12-3	10.9	-0.650	0.00575	0.000498
16-1	10.9	0.000	0.00616	0.000529
16-2	10.9	0.330	0.00585	0.000562
17-1	10.9	0.000	0.00612	0.000527
17-2	10.9	0.655	0.00538	0.000564
17-3	10.9	-0.981	0.00571	0.000492
18-1	10.9	0.000	0.00605	0.000520
18-2	10.9	0.850	0.00500	0.000554
18-3	10.9	-0.737	0.00591	0.000491
19-1	10.9	0.000	0.00608	0.000521
19-2	10.9	0.525	0.00560	0.000563
19-3	10.9	0.514	0.00565	0.000565
19-4	10.9	-0.217	0.00610	0.000494
19-5	10.9	-0.218	0.00603	0.000512
20-1	10.9	0.000	0.00607	0.000517
20-2	10.9	0.389	0.00581	0.000564
20-3	10.9	0.404	0.00578	0.000565
20-4	10.9	-0.221	0.00612	0.000499
20-5	10.9	-0.220	0.00609	0.000513
21-1	10.9	0.000	0.00610	0.000528
21-2	10.9	0.123	0.00610	0.000546
21-3	10.9	0.114	0.00608	0.000544
21-4	10.9	0.091	0.00611	0.000541
21-5	10.9	0.120	0.00606	0.000544
22-1	10.9	0.000	0.00617	0.000516
22-2	10.9	0.344	0.00586	0.000562
23-1	10.9	0.000	0.00612	0.000526
23-2	10.9	0.303	0.00595	0.000555
23-3	10.9	0.217	0.00601	0.000551
23-4	10.9	0.214	0.00601	0.000551
24-1	10.9	0.000	0.00606	0.000515
24-2	10.9	0.108	0.00610	0.000536
24-3	10.9	0.105	0.00609	0.000539
24-4	10.9	0.106	0.00609	0.000539
24-5	10.9	0.105	0.00604	0.000540
25-1	10.9	0.000	0.00611	0.000515
25-2	10.9	0.166	0.00601	0.000534
25-3	10.9	0.167	0.00604	0.000545
25-4	10.9	0.076	0.00612	0.000534
27-1	10.9	0.000	0.00624	0.000528
27-2	10.9	0.056	0.00603	0.000524
27-3	10.9	0.057	0.00613	0.000525
27-4	10.9	0.055	0.00621	0.000529
27-5	10.9	0.054	0.00622	0.000533
27-6	10.9	0.056	0.00617	0.000531
27-7	10.9	0.055	0.00611	0.000526
27-8	10.9	0.051	0.00604	0.000522